

Proceedings

Key Features of Solid Lipid Nanoparticles Prepared with Nanoclay and Spring Water Ingredients with Demonstrated Wound Healing Activity: A Pilot Study [†]

Fátima García-Villén ¹, Rita Sánchez-Espejo ², Ana Borrego-Sánchez ², Pilar Cerezo ¹, Raquel de Melo Barbosa ³ and César Viseras ^{1,2}

¹ Department of Pharmacy and Pharmaceutical Technology, Faculty of Pharmacy. University of Granada, Campus of Cartuja, 18071 s/n Granada, Spain; mcerezo@ugr.es (P.C.); cviseras@ugr.es (C.V.)

² Andalusian Institute of Earth Sciences, CSIC-UGR. Avenida de las Palmeras 4, 18100 Armilla, Granada, Spain; ext.risanchez@ugr.es (R.S.-E.); anaborrego@iact.ugr-csic.es (A.B.-S.)

³ Department of Pharmacy, University of Rio Grande do Norte, Natal. Gal Gustavo C Farias street, s/n, Natal 59078-970 Brazil; m.g.barbosafernandes@gmail.com

* Correspondence: fgarvillen@ugr.es; Tel.: +34-608356567

[†] Presented at the 1st International Electronic Conference on Pharmaceutics, 1–15 December 2020; Available online: <https://iecp2020.sciforum.net/>.

Published: date

Abstract: Solid Lipid Nanoparticles (SLN) emerged in the late 20th century as versatile nanoparticle drug delivery systems. Since then, SLNs have demonstrated to be very useful for the encapsulation of a great number of actives. In particular, the role of SLN in wound healing is pretty recent, since the major part of scientific literature on this field is concentrated during 2019 and 2020. In this pilot study we propose the formulation of a semisolid system formed by SLN embedded in an inorganic hydrogel with demonstrated wound healing activity. The hot emulsification method was used to prepare the SLN. Subsequently, the SLN were embedded in a wound healing hydrogel composed of a clay mineral (PS9) and a natural spring water (ALI). Granulometry, pH, rheology and TEM microscopy were used to characterize the formulations. Results showed that the use of natural spring water does not affect the SLN's particle size unlike PS9, which increased them. TEM microphotographs revealed that this increase in particle size was due to SLN coalescence in presence of PS9. The pH of all samples was stable for 3 months. Rheology was significantly influenced by the aqueous medium, better results obtained with ALI. In conclusion, despite of the necessity of some improvements, the proposed SLN formulation would be very versatile for wound healing due to the possibility to load different actives inside the SLN together with the wound healing activity of the PS9/ALI hydrogel.

Keywords: solid lipid nanoparticles; sepiolite; spring water; hot emulsification

1. Introduction

Solid Lipid Nanoparticles (SLN) emerged in the late 20th century as versatile nanoparticle drug delivery systems. They consist of a room-temperature-solid lipid droplets surrounded by a surfactant and dispersed in water. The particularity of SLNs respect to other lipidic systems is the fact that the lipid molecules are solid at room temperature.

Since their origin, SLNs have demonstrated to be useful for the encapsulation of a great number of actives [1–5]. In particular, the role of SLN in wound healing is pretty recent, since the major part

of scientific literature on this field is concentrated during 2019 and 2020, as reflected by the results obtained in the main databases (keywords “solid lipid nanoparticle” and “wound healing”; Boolean operator “and”; databases: Web of Sciences, Science Direct and Pubmed). In these recent papers, daptomycin, curcumin, cefadroxil, melatonin, chamomile oil, propolis, calendula officinalis extract and silver sulfadiazine are some of the proposed active ingredients exerting wound healing activity [6–13]. As it can be seen, the major part of the proposed actives have a natural origin, demonstrating the current popularity of natural actives in dermatology. Moreover, the very same SLNs could exert positive skin effects, since the lipid can form a coherent film over the skin after their application, thus restoring the damaged protective lipid film of the skin [1,14].

The use of inorganic ingredients on wound healing has been addressed in a deeper way [15], although it continues to grow nowadays. Wound healing properties of fibrous clay minerals/spring water hydrogels have been recently reported [16,17], together with the safety of the ingredients in terms of hazardous elements release [18]. In these studies, the importance of the formulative studies has been highlighted, since neither the spring waters nor the clay minerals by themselves were able to improve *in vitro* wound closure as much as the resultant hydrogels did.

All that being said, the present pilot study explores the main characteristics of a hybrid semisolid system formed by SLN embedded in an inorganic hydrogel made of spring water and a fibrous clay mineral with wound healing activity [16]. The ultimate aim is to develop a semisolid formulation able to improve wound healing both by enhancing fibroblast mobility and proliferation together with an additional wound healing activity which would be provided by the actives loaded into the SLN. Due to the elemental richness of the spring water and the clay mineral, the stability and main properties of SLN system should be addressed, thus studying the possible interactions between the ingredients and their effects. To do so, rheology, pH, particle size and Transmission Electron Microscopy (TEM) microscopy of the prepared formulations were analysed and compared.

2. Experiments

2.1. Materials

Crodamol™ CP or cetyl palmitate (> 98% of purity; 480.85 g/mol; $T_f = 55\text{--}56\text{ °C}$) was kindly gifted by CRODA International Plc. Kolliphor® was purchased from Sigma-Aldrich and natural spring water (ALI) was obtained from Alicún de las Torres thermal station, located in Granada, Spain. Elemental composition of ALI has been deeply addressed by García-Villén et al. [18,19] and Prado-Pérez et al. [20], among others. Briefly, ALI water is specially rich in calcium, magnesium and sulphur and possesses a pH of 7.9 and a conductivity of 2251.5 $\mu\text{S/cm}$. The clay mineral (PS9) is a fibrous clay called sepiolite, which has also been fully characterized in previous studies [19]. PS9 was kindly gifted by TOLSA GROUP (Madrid, Spain) and contains 92% w/w of sepiolite and around an 8% w/w of muscovite.

2.2. Methods

2.2.1. Formulation Procedure

SLN were obtained by means of the hot ultrasonication method. Aqueous and oleous phases were measured and warmed up (approximately 60 °C) separately. The aqueous phase was formed by 10% w/w of Kolliphor® and 80% w/w of milliQ® or ALI water. The oleous phase was formed by 10% w/w of cetyl palmitate, which passed from solid to liquid during the warming up (until 60 °C). At this point, the A/O emulsion was obtained by the addition of the aqueous phase to cetyl palmitate under high speed agitation provided by an Ultra-Turrax® apparatus (15000 rpm, 3 min). Subsequently, ultrasonication was performed for 15 min working under a constant 20% duty cycle. Next, the emulsion was rapidly cooled in an ice bath to induce the crystallization of cetyl palmitate goticles, thus forming SLN. This procedure gave rise to two types of formulations, depending on the type of water used for the aqueous phase: SLN@milliQ and SLN@ALI. Two additional formulations were obtained after the addition of 5% w/w of PS9. The clay mineral was incorporated into the

aforementioned formulations right after the obtention and cooling of the SLN system. Homogenization was obtained by Ultra-Turrax® (13000 rpm, 5 min), thus giving rise to either SLN@ALI@PS9 and SLN@milliQ@PS9 formulations.

2.2.2. Characterization of the Prepared Formulations

Formulations were assessed and compared by means of rheology, pH measurements, particle size analysis and Transmission Electron Microscopy (TEM). All the characterizations were performed at predefined time intervals from the preparation of the formulations: 1 week (1w), 15 days (15d) and 2 months (2m), except for TEM, which was done once (15d).

Rheology studies were performed by means of a Thermo Scientific HAAKE apparatus (RotoVisco 1) equipped with a serrated plate/plate sensor system (Ø 20 mm PPS20S). Flow curves of all the formulations were obtained from 70 s⁻¹ to 800 s⁻¹ at a constant temperature of 25 °C (± 0.5 °C) provided by a LT ecocool™ 100 temperature controller (Clever Scientific Ltd., UK).

Since the formulations are intended to be applied to wounded skin, the pH was measured and monitored in order to detect possible chemical instability. Crison pH25+ device equipped with a semisolid electrode (5053T) was used to measure pH.

Particle size of all the formulations was analyzed by a Marvern Mastersizer 2000 LF granulometer (Malvern Instruments™). Formulations were dispersed in purified water until optimal laser obscuration degree was obtained (fixed at 10–20%, indicated at real-time by the Mastersizer 2000 software). Each experiment was performed in triplicate and the SPAN factor calculated (Equation (1)).

$$\text{SPAN} = \frac{d_{90}-d_{10}}{d_{50}} \quad (1)$$

Prior to the TEM analysis, formulations were diluted in ultrapurified water (milliQ® grade) as required (1:50 or 1:100) and placed over formvar/SiO coated copper grids (200 mesh). Uranyl acetate (1%, pH 7) was dropped onto the grid for sample negative staining, the excess removed after 1 min. Subsequently, samples were left to dry at room temperature. TEM microphotographs were obtained in a Carl Zeiss SMT microscope (LIBRA 120 PLUS), equipped with a lanthanum hexaboride filament.

3. Results and Discussion

3.1. Rheology Studies

Flow curves obtained during the rheology study are shown in Figure 1. The presence of PS9 produced significant differences. SLN@ALI and SLN@milliQ showed a Newtonian-like profile, though with high fluctuations, whereas SLN@ALI@PS9 and SLN@milliQ@PS9 displayed a non-Newtonian pseudoplastic behavior. For the latter, the flow curves profiles were in agreement with those previously reported for PS9 hydrogels (without SLN) [19]. The influence of SLN can be observed due to the rheopectic profile of SLN@milliQ@PS9 and SLN@ALI@PS9 with respect to PS9/ALI hydrogels [19], that reported to be thixotropic. Likewise, the type of water in SLN@ALI@PS9 and SLN@milliQ@PS9 influenced the final viscosity of the system, ALI water increasing this value with respect to the milliQ® system. No remarkable differences were detected in the studied time lapse (data not shown).

3.2. pH

SLN@milliQ and SLN@ALI showed a lower pH (around 6) with respect to SLN@milliQ@PS9 and SLN@ALI@PS9, which possessed a pH between 7 and 8 (Figure 2). The presence of PS9 increased the pH value towards the its natural value due to the intrinsic buffer activity of phyllosilicates.

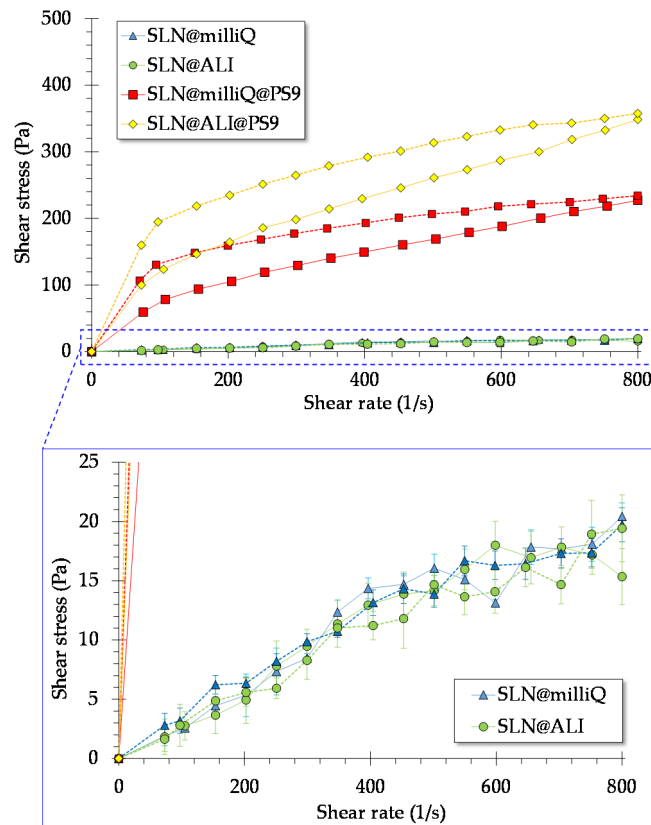


Figure 1. Flow curves of SLN@milliQ, SLN@milliQ@PS9, SLN@ALI and SLN@ALI@PS9. Uphill curves ($70\text{--}800\text{ s}^{-1}$) are represented with a continuous line, while dashed lines were used for the return flow curves ($800\text{--}70\text{ s}^{-1}$).

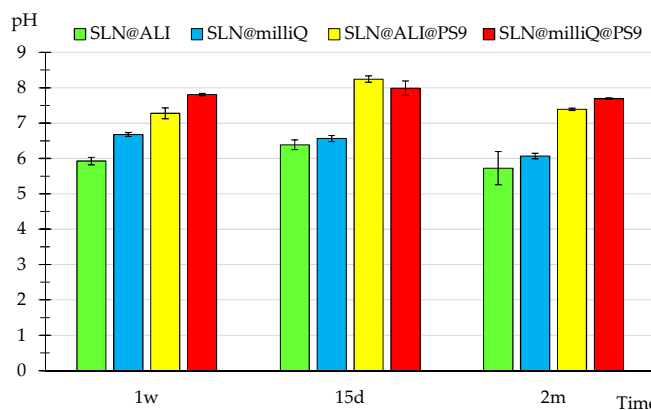


Figure 2. pH of the formulations through time (mean values \pm s.d.; $n = 8$).

3.3. Particle Size

Particle size results are shown in Figure 3. SLN@milliQ and SLN@ALI had a particle size between 0.3 and $0.04\text{ }\mu\text{m}$, the main mode being $0.15\text{ }\mu\text{m}$. These particle sizes maintained stable form 2 months (data not shown). Moreover, the type of water did not influence the resultant particle size of the SLNs (SLN@milliQ_1w and SLN@ALI_1w, overlapped curves, Figure 3), thus demonstrating that ALI water is completely valid for the formulation of SLNs.

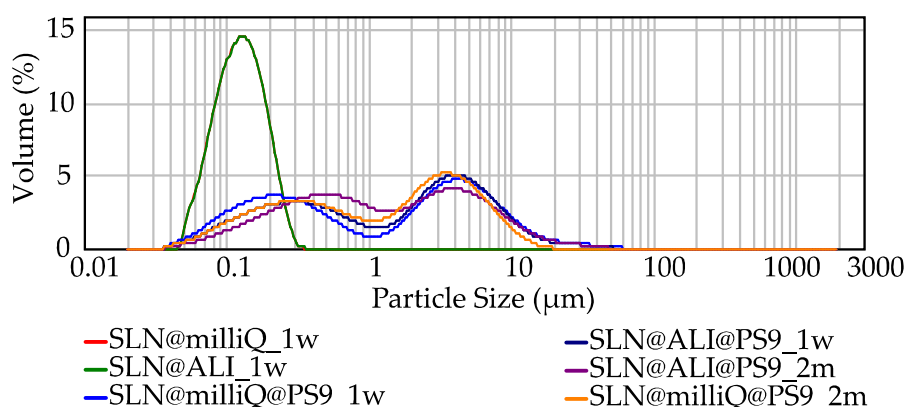


Figure 3. Particle size analysis of formulations. For simplicity, the most relevant results of 1 w and 2 m samples are shown (mean sizes; $n = 3$).

On the other hand, the presence of PS9 clearly influenced the final SLN particle sizes. As it can be seen in the figure and corroborated by the SPAN factor (Table 1). Two modes appeared in SLN@ALI@PS9 and SLN@milliQ@PS9 (either 1 w and 2 m). The biggest mode could be ascribed to the presence of PS9 particles, as reported in previous studies [16], while the smaller one would be ascribed to the SLN. We hypothesize that the size changes of SLN caused by PS9 could be due to the adsorption of the tensioactive to the clay mineral surface. Further studies should be performed in order to confirm this hypothesis.

Table 1. Statistical particle size analysis.

Sample	d_{10} (μm)	d_{50} (μm)	d_{90} (μm)	SPAN Factor
SLN@milliQ_1w	0.073	0.124	0.202	1.041
SLN@ALI_1w	0.074	0.124	0.203	1.042
SLN@milliQ@PS9_1w	0.116	1.595	8.277	5.116
SLN@ALI@PS9_1w	0.141	1.776	7.747	4.283
SLN@ALI@PS9_2m	0.180	1.235	7.650	6.046
SLN@milliQ@PS9_2m	0.142	1.435	6.143	4.181

3.4. TEM

Microphotographs of the samples are summarized in Figure 4. As expected, Figure 4A,B correspond to SLN@ALI and SLN@milliQ, respectively. Consequently, no clay particles fibers were found and the dimensions of the SLN are in agreement with the particle sizes reported. Coalescence of SLN nanoparticles is visible in both SLN@ALI@PS9 (Figure 4C) and SLN@milliQ@PS9 (Figure 4D), thus explaining the increase in particle size results. One of the main features of clay minerals is their high surface area. We hypothesize that the presence of the clay particles could alter the dimensions of the SLN due to adsorption of the surfactant molecules by the clay fibers. In fact, a concentrated zone was found in sample SLN@milliQ@PS9 (Figure 4D). In this area, sepiolite fibers area are surrounded by tiny particles of around 30 nm (see arrows in Figure 4D). In view of the sizes and the aspect of these “particles”, they can be identified as micelles formed by the concentration of surfactant molecules over the sepiolite particles. This result is in agreement with the hypothesis explaining the coalescence of the SLNs.

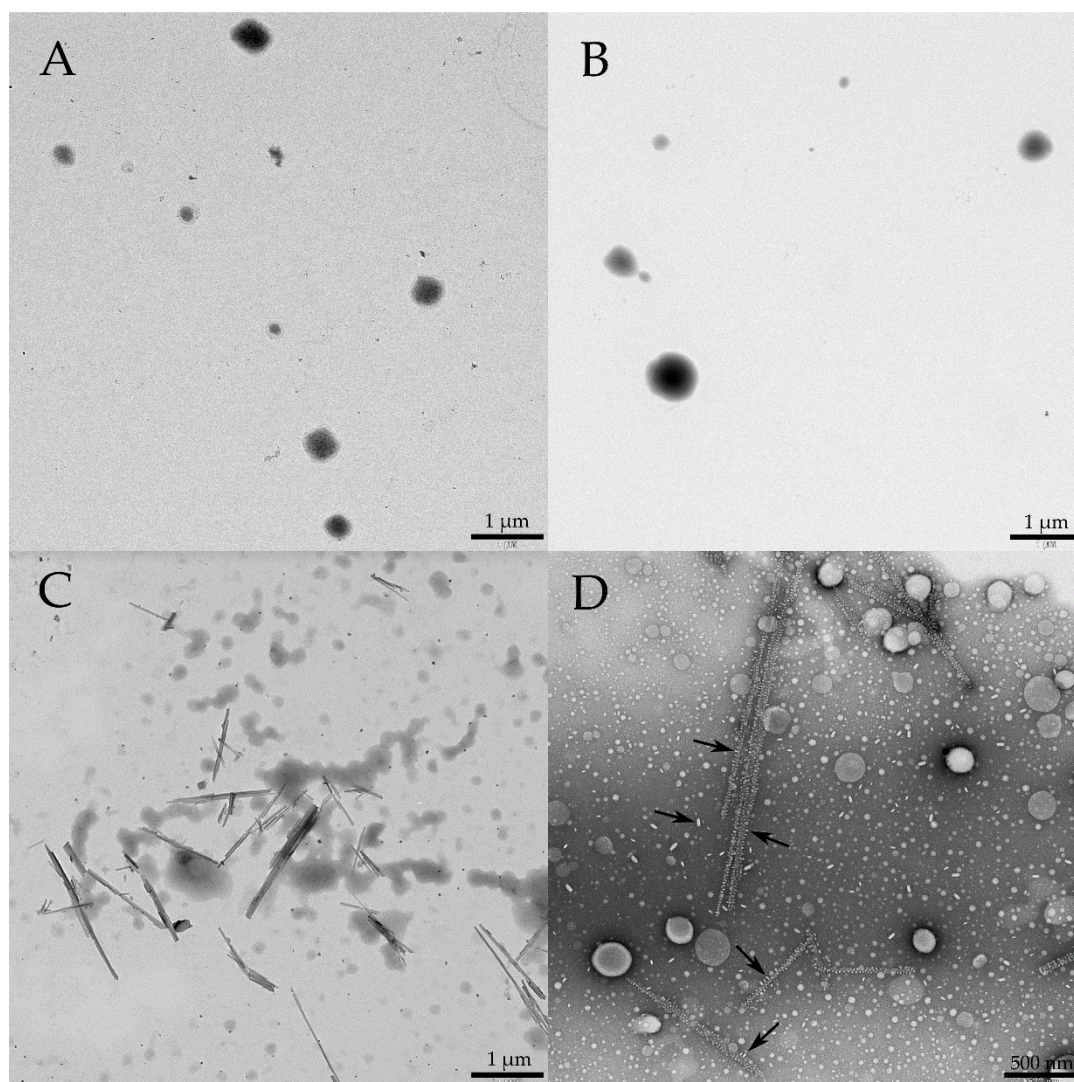


Figure 4. Microphotographs obtained during TEM studies of the formulations. (A) SLN@ALI; (B) SLN@milliQ; (C) SLN@ALI@PS9; (D) SLN@milliQ@PS9. Arrows mark tiny micelles surrounding sepiolite fibers.

5. Conclusions

This pilot study explores the main characteristics of a hybrid semisolid system formed by SLN embedded in an inorganic hydrogel made of spring water and a fibrous clay mineral. This kind of formulation would be very versatile for the treatment of skin diseases, specifically for wound healing, due to the possibility to load different actives inside the SLN together with the already demonstrated wound healing activity of the inorganic hydrogel. The results demonstrated that final particle size of SLN was not influenced by the use of Alicún de las Torres spring source. Nonetheless, the adsorption of surfactant molecules by the clay mineral particles induced coalescence of SLN, thus altering the final features of the formulation. Despite this inconvenience and the necessity of further studies, the formulations reported promising stability and rheological properties.

Author Contributions: Data curation, F.G.-V.; Funding acquisition, C.V.; Methodology, F.G.-V., R.d.M.B.; Project administration, C.V.; Supervision, R.d.M.B; Writing—original draft, F.G.-V.; Writing—review & editing, A.B.-S., R.S.-E., P.C. All authors have read and agreed to the published version of the manuscript.

Acknowledgments: This research was funded by Ministerio de Ciencia e Innovación, CGL2016–80833-R; Consejería de Economía, Innovación, Ciencia y Empleo, Junta de Andalucía, P18-RT-3786 and Ministerio de Educación, Cultura y Deporte, FPU15/01577.

Conflicts of Interest: The authors declare no conflict of interest.

References

1. Müller, R.H.; Mäder, K.; Gohla, S. Solid lipid nanoparticles (SLN) for controlled drug delivery—A review of the state of the art. *Eur. J. Pharm. Biopharm.* **2000**, *50*, 161–177.
2. Battaglia, L.; Gallarate, M. Lipid nanoparticles: State of the art, new preparation methods and challenges in drug delivery. *Expert Opin. Drug Deliv.* **2012**, *9*, 497–508.
3. Muller, R.H.; Keck, C.M. Challenges and solutions for the delivery of biotech drugs—A review of drug nanocrystal technology and lipid nanoparticles. *J. Biotechnol.* **2004**, *113*, 151–170.
4. Barbosa, R.M.; Da Silva, C.M.G.; Bella, T.S.; De Araújo, D.R.; Marcato, P.D.; Durán, N.; De Paula, E. Cytotoxicity of solid lipid nanoparticles and nanostructured lipid carriers containing the local anesthetic dibucaine designed for topical application. *J. Phys. Conf. Ser.* **2013**, 429.
5. De Araújo, D.R.; Da Silva, D.C.; Barbosa, R.M.; Franz-Montan, M.; Cereda, C.M.; Padula, C.; Santi, P.; De Paula, E. Strategies for delivering local anesthetics to the skin: Focus on liposomes, solid lipid nanoparticles, hydrogels and patches. *Expert Opin. Drug Deliv.* **2013**, *10*, 1551–1563.
6. Sarecka-Hujar, B.; Banyś, A.; Ostróžka-Cieślik, A.; Balwierz, R.; Dolińska, B. Evaluation of the potential of nanoparticles containing active substances in selected chronic diseases. *Adv. Clin. Exp. Med.* **2020**, *29*, 385–397.
7. Romić, M.D.; Sušac, A.; Lovrić, J.; Cetina-Čizmek, B.; Filipović-Grčić, J.; Hafner, A. Evaluation of stability and in vitro wound healing potential of melatonin loaded (lipid enriched) chitosan based microspheres. *Acta Pharm.* **2019**, *69*, 635–648.
8. Gad, H.A.; Abd El-Rahman, F.A.A.; Hamdy, G.M. Chamomile oil loaded solid lipid nanoparticles: A naturally formulated remedy to enhance the wound healing. *J. Drug Deliv. Sci. Technol.* **2019**, *50*, 329–338.
9. Rosseto, H.C.; de Toledo, L.A.S.; de Francisco, L.M.B. de Esposito, E.; Lim, Y.; Valacchi, G.; Cortesi, R.; Bruschi, M.L. Nanostructured lipid systems modified with waste material of propolis for wound healing: Design, in vitro and in vivo evaluation. *Colloids Surf. B Biointerfaces* **2017**, *158*, 441–452.
10. Mishra, R.K.; Ramasamy, K.; Lim, S.M.; Ismail, M.F.; Majeed, A.B.A. Antimicrobial and in vitro wound healing properties of novel clay based bionanocomposite films. *J. Mater. Sci. Mater. Med.* **2014**, *25*, 1925–1939.
11. Garcia-Orue, I.; Gainza, G.; Girbau, C.; Alonso, R.; Aguirre, J.J.; Pedraz, J.L.; Igartua, M.; Hernandez, R.M. LL37 loaded nanostructured lipid carriers (NLC): A new strategy for the topical treatment of chronic wounds. *Eur. J. Pharm. Biopharm.* **2016**, *108*, 310–316.
12. Sandri, G.; Bonferoni, M.C.; D’Autilia, F.; Rossi, S.; Ferrari, F.; Grisoli, P.; Sorrenti, M.; Catenacci, L.; Del Fante, C.; Perotti, C.; et al. Wound dressings based on silver sulfadiazine solid lipid nanoparticles for tissue repairing. *Eur. J. Pharm. Biopharm.* **2013**, *84*, 84–90.
13. Arana, L.; Salado, C.; Vega, S.; Aizpurua-Olaizola, O.; Arada, I.; de la Suarez, T.; Usobiaga, A.; Arrondo, J.L.R.; Alonso, A.; Goñi, F.M.; et al. Solid lipid nanoparticles for delivery of Calendula officinalis extract. *Colloids Surf. B Biointerfaces* **2015**, *135*, 18–26.
14. De Vringer, T.; De Ronde, H.A.G. Preparation and structure of a water-in-oil cream containing lipid nanoparticles. *J. Pharm. Sci.* **1995**, *84*, 466–472.
15. García-Villén, F.; Souza, I.M.S.; de Melo Barbosa, R.; Borrego-Sánchez, A.; Sánchez-Espejo, R.; Ojeda-Riascos, S.; Viseras, C. Natural inorganic ingredients in wound healing. *Curr. Pharm. Des.* **2020**, *26*, 621–641.
16. García-Villén, F.; Faccendini, A.; Miele, D.; Ruggeri, M.; Sánchez-Espejo, R.; Borrego-Sánchez, A.; Cerezo, P.; Rossi, S.; Viseras, C.; Sandri, G. Wound healing activity of nanoclay/spring water hydrogels. *Pharmaceutics* **2020**, *12*, 1–24.
17. García-Villén, F.; Sánchez-Espejo, R.; Borrego-Sánchez, A.; Cerezo, P.; Cucca, L.; Sandri, G.; Viseras, C. Correlation between elemental composition/mobility and skin cell proliferation of fibrous nanoclay/spring water hydrogels. *Pharmaceutics* **2020**, *12*, 1–20.
18. García-Villén, F.; Sánchez-Espejo, R.; Borrego-Sánchez, A.; Cerezo, P.; Perioli, L.; Viseras, C. Safety of nanoclay/spring water hydrogels: Assessment and mobility of hazardous elements. *Pharmaceutics* **2020**, *12*, 1–17.
19. García-Villén, F.; Sánchez-Espejo, R.; López-Galindo, A.; Cerezo, P.; Viseras, C. Design and characterization of spring water hydrogels with natural inorganic excipients. *Appl. Clay Sci.* **2020**, *197*, 105772.
20. Prado-Pérez, A.J.; Pérez del Villar, L. Dedolomitization as an analogue process for assessing the long-term behaviour of a CO₂ deep geological storage: The Alicún de las Torres thermal system (Betic Cordillera, Spain). *Chem. Geol.* **2011**, *289*, 98–113.

Publisher's Note: MDPI stays neutral with regard to jurisdictional claims in published maps and institutional affiliations.

© 2020 by the authors; licensee MDPI, Basel, Switzerland. This article is an open access article distributed under



the terms and conditions of the Creative Commons by Attribution (CC-BY) license (<http://creativecommons.org/licenses/by/4.0/>).